The Thesis Committee for Harold J. Johnson
certifies that this is the approved version of the following thesis:

NUMERICAL CALCULATIONS OF THE DECAY RATE OF A FALSE VACUUM FOR A MODIFIED QUARTIC POTENTIAL

SUPERVISING COMMITTEE:

Sonia Paban, Supervisor

Can Kilic

NUMERICAL CALCULATIONS OF THE DECAY RATE OF A FALSE VACUUM FOR A MODIFIED QUARTIC POTENTIAL

by

Harold J. Johnson

Thesis

Presented to the Faculty of the Graduate School of

The University of Texas at Austin

in Partial Fulfillment

of the Requirements

for the Degree of

Master of Arts

The University of Texas at Austin

December 2023

Acknowledgments

I would like to thank my advisor, Sonia Paban, for permitting me to perform research with her group at University of Texas at Austin, for providing her mentorship and support along the way. Thank you also Dr. Can Kilic for the reading of my Thesis as well as providing guidance along the way to the completion of my program.

Preface

Readers, this document represents a great deal of time and effort. Enjoy. Cheers, Harold J. Johnson.

Abstract

NUMERICAL CALCULATIONS OF THE DECAY RATE OF A FALSE VACUUM FOR A MODIFIED QUARTIC POTENTIAL

Harold J. Johnson, MA
The University of Texas at Austin, 2023

SUPERVISOR: Sonia Paban

The possibility of two or more vacuum states with different energy densities is a common feature of many potentials. The classical state is in stable equilibrium at any of these minima but is made unstable by quantum effects. The formalism that describes transitions from a false (higher energy density) vacuum to a true (lowest energy density) vacuum was developed decades ago. It suggests that false vacuum decay occurs via a quantum tunneling process, with the nucleation of a bubble of true vacuum, which, as it expands, transforms the metastable false vacuum into the more stable phase. The well-known procedure to calculate the tunneling rate uses an Euclidean Bounce solution. However, some potentials exist for which this method doesn't work. All these potentials are unbounded from below, and hence don't have a proper true vacuum. Instead of a single bounce, these potentials have either an infinite family of bounces with identical tunneling rates or no bounce solution.

In this thesis, we investigate these phenomena. Since potentials are only known in finite regions of field space, we approximate the known unbounded potential with

a series of potentials bounded from below and for which the tunneling rate is well-defined. We compute the change in the tunneling rate as the field space distance and the energy density distance between the true and false vacua increases.

We find that neither our numerical calculation of a modified quartic potential, nor the method of "Pseudo-Bounce", provide a reliable path for the calculation of the decay rate of the false vacuum. If $-\lambda\phi^4$ is only an effective potential for small values of ϕ, our numerical analysis shows that we must know the actual potential to estimate both the decay path and the decay rate. Espinosa et al.'s approach never agrees with the numerical result.

Table of Contents

List of Tables

List of Figures

Chapter 1: Introduction

The false vacuum decay picture has been around for decades. It was first developed by Kobzarev et al. (1974) and quickly followed up on by Callan and Coleman (1977) with a treatment that has seen predominant usage. The interest in the subject ranges from conjectures about the ultimate cosmological fate of the universe to string theories. In the standard model, it has been speculated whether the electroweak vacuum is metastable; if it is, then the universe could have experienced a first-order phase transition prior to our current epoch, making the prior era one with a different set of physics Chigusa et al. (2023). In cosmology, it has been speculated that our universe could have been one that settled from its early hot and dense state, in which it was very far from an energy minimum to a false vacuum state as it cooled. Others Okun (1996) have speculated that our universe may itself be now in a local false vacuum region, which could suddenly decay to a true vacuum and if this were to happen it would have destructive consequences. The false vacuum decay process is analogous to that of bubble nucleation in statistical physics, where bubbles in a heated fluid can occasionally grow to a size where it is energetically favorable for it to continue to grow and eventually evaporate the volume of fluid contained; a similar process is speculated but instead with quantum fluctuations rather than thermal, which could lead to a false vacuum conversion into a true vacuum state. This runaway process means that the universe could suddenly decay from a false vacuum into a true vacuum, converting all of space into true vacuum within the expanding bubble radius, in the process possibly changing cosmological parameters and the structure of elementary particles and their resultant fundamental forces, potentially destroying the universe... giving future generations another reason for societal angst.

Let's start with the quantum field theory of a scalar field in 4D spacetime:

$$L = \partial_\mu \phi \partial^\mu \phi - V(\phi) \tag{1.1}$$

Let V (ϕ) have two unequal relative minima, one of which is a local minimum ϕ^+ and one is an absolute minimum ϕ^-. The field for which ϕ equals ϕ^+ is a classical equilibrium state we call the false vacuum; ϕ^- is a classical equilibrium state of lowest energy, called true vacuum. In classical mechanics, there can be multiple local minima; in quantum mechanics, tunneling can cause one of these local minima to move to a lower energy state. What we want to compute is the probability of decay of the false vacuum per unit volume per unit time, Γ/V.

We'll start by reviewing this formalism developed by Coleman and Callan, in computing the probability of decay which incorporate what are known as Euclidean bounce solutions, using the 'undershoot-overshoot' argument. However, following the work of Espinosa (2019), we will find that there exists a class of potentials for which these bounce solutions do not work, which are called "Fubini bounces" from Fubini's solution Fubini (1976). The class of quartic potentials $V = -\lambda\phi^4$ have the property that solutions to the Euler-Lagrange equations with arbitrary initial conditions 0 are all bounces. We will also discuss variations of these $-\lambda\phi^4$ potentials for which there are no bounce solutions, as shown by Espinosa. Finally, we will investigate the breakdown of this class of solutions, by using our own modified $-\lambda\phi^4$ potential and numerically comparing its bounce solutions to the more generic known class. Each of these formalisms between the standard Euclidean bounce and the Fubini Bounces aims to produce a method to calculate the decay rate of a false vacuum. If our numerical calculation can produce the same result as Espinosa's analytical result, then

we will have a straightforward method for calculating the decay of these classes of potentials.

Chapter 2: Euclidean Bounce Formalism

2.1 1D particle moving in an uneven double-well potential

Consider a particle moving in one dimension with the Lagrangian

$$L = \frac{1}{2}q^2 - V(q) \tag{2.1}$$

with a potential as in [Figure 2.1]. There is no quantum minimum that corresponds to the classical minimum ϕ_{fv}. In the WKB semi-classical approximation the particle penetrates the potential barrier V and materializes at α with zero kinetic energy, after which it propagates classically. The decay width associated with this process is given by the expression

$$\Gamma = A\ e^{-B/\hbar} \tag{2.2}$$

where

$$B = \int_0^{\alpha} dq\sqrt{2V} \tag{2.3}$$

To generalize the description of a particle moving in multiple dimensions we want to construct a vector q . The Lagrangian for this is

$$L = \frac{1}{2}\frac{d\vec{q}}{dt}\frac{d\vec{q}}{dt} - V(\vec{q}) \tag{2.4}$$

Like the 1D case V(q) is assumed to have a local minimum at q_0 and the zero of the energy is chosen such that $V(q_0)$ vanishes. The single other zero of V in the 1D case, α , is replaced by a surface of zeros, σ, which is a barrier. Here also

$$B = \int_{\vec{q_0}}^{\vec{\alpha}} ds\sqrt{2V} \tag{2.5}$$

where

$$(ds)^2 = d\vec{q}\cdot d\vec{q} \tag{2.6}$$

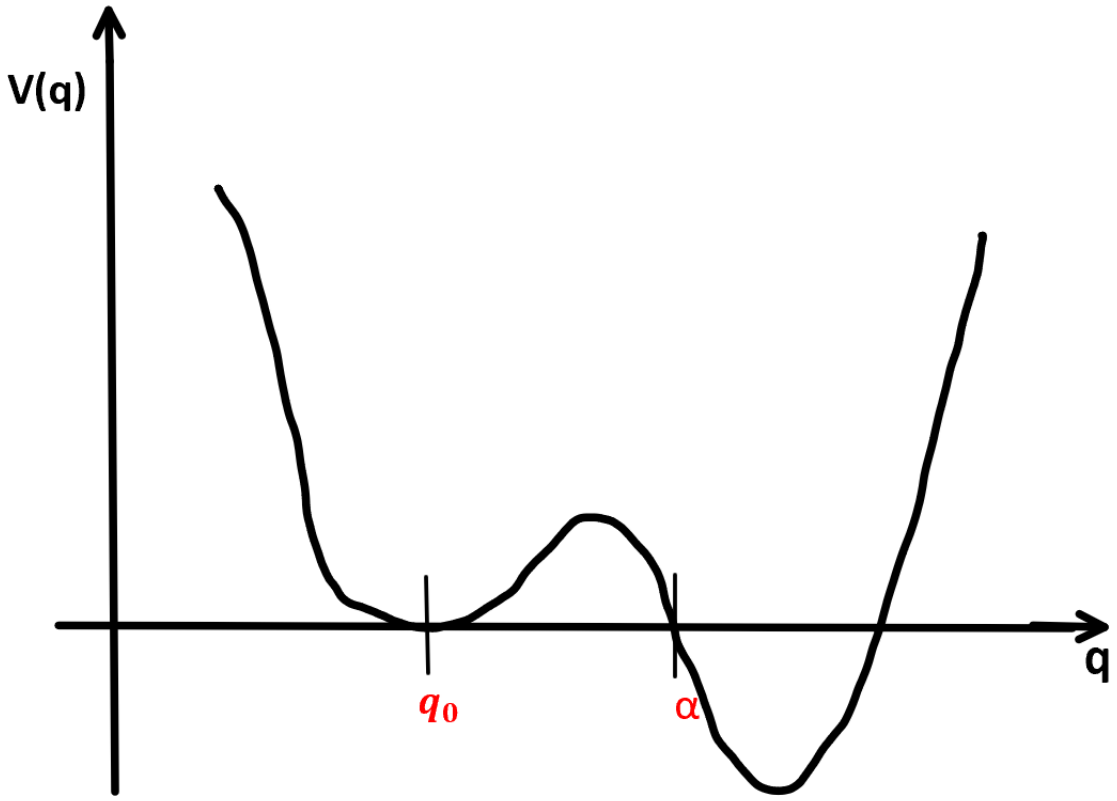

Figure 2.1: A Double well potential V

α is a point on σ and the integral is over a path for which B is an extrema

$$\delta \int_{\vec{q_0}}^{\vec{\alpha}} dq\sqrt{2V} = 0 \tag{2.7}$$

so the particle penetrates the barrier along the path of least resistance. The particle will penetrate the barrier, emerging with zero kinetic energy and propagate classically. We can recast these formulae in the form of Euler-Lagrange equations for more convenience. It is known that the solution to the variational problem with fixed end points,

$$\delta \int ds\sqrt{2(E-V)} = 0 \tag{2.8}$$

are paths in configuration space traced by solutions to these equations

$$\frac{d\vec{q}^2}{dt^2} = -\frac{\partial V}{\partial q} \tag{2.9}$$

with

$$\frac{1}{2}\frac{d\vec{q}}{dt}\cdot\frac{d\vec{q}}{dt} + V = E \tag{2.10}$$

The variational problem (2.7) is of this form except E is zero, the sign of V is negative, and the end-point, α, is free to vary along the surface of zeroes, σ. If we temporarily ignore this last point and fix $\vec{\alpha}$ then solutions to our variational problem are paths traced in configuration space by solutions to the following differential equation:

$$\frac{d^2\vec{q}}{d\tau^2} = -\frac{\partial V}{\partial \vec{q}} \tag{2.11}$$

with

$$\frac{1}{2}\frac{d\vec{q}}{d\tau}\cdot\frac{d\vec{q}}{d\tau} - V = 0 \tag{2.12}$$

Notice that (2.11) is simply the imaginary time version of (2.9), which takes us from Minkowski to Euclidean space and $\tau = it$; the Euler-Lagrange equation for the imaginary time version of Hamilton's principle

$$\delta \int d\tau L_E = 0 \tag{2.13}$$

where

$$L_E = \frac{1}{2}\frac{d\vec{q}}{d\tau}\cdot\frac{d\vec{q}}{d\tau} - V \tag{2.14}$$

By (2.12) the classical equilibrium point, q_0, can only be reached asymptotically, as τ goes to minus infinity,

$$\lim_{\tau\to-\infty}\vec{q} = \vec{q_0} \tag{2.15}$$

Using time translation invariance, let's choose the imaginary time at which the particle reaches to be $\tau = 0$. At $\tau = 0$, again by (2.12), $dq/d\tau$ vanishes,

$$\left.\frac{d\vec{q}}{dt}\right|_0 = 0 \tag{2.16}$$

and

$$\int_{\vec{q_0}}^{\vec{\sigma}} ds\sqrt{2V} = \int_{-\infty}^{0} d\tau L_E = 0 \tag{2.17}$$

By (2.16), the variation of this expression with respect to changes in vanishes; we no longer require the condition that be fixed. (2.16) also tells us that the motion of the particle for positive τ is the time-reversal of its motion for negative τ; the particle bounces off σ at $\tau = 0$ and returns to q_0 at $\tau = +\infty$. This motion we call a "bounce". The coefficient B is the total Euclidean action for the bounce

$$B = \int_{-\infty}^{\infty} d\tau L_E \stackrel{\text{def}}{=} S_E \tag{2.18}$$

Thus, to find the coefficient B, we need only find the bounce, the solution of the imaginary-time equations of motion obeying boundary conditions (2.15) and (2.16). Eq (2.12) is a consequence of the equations of motion and (2.15). However, the bounce must really reach the surface at $\tau = 0$; in other words, a position from which a classical particle, released at rest, can escape to infinity. Thus the trivial solution

to the equations, constant q, is not allowed. In the case that there are numerous bounces, the preferred one is the one which minimizes the Euclidean action. There may be many bounces with the same Euclidean action; in this case we must sum the contributions to Γ of all these bounces.

2.2 Barrier Penetration in Field Theory

Let's translate the mechanics of the previous section and a 1D particle, to that of field theory. Here is our Euclidean equation of motion

$$(\frac{\partial^2}{\partial\tau^2} + \nabla^2)\phi = V'(\phi) \tag{2.19}$$

where the ' denotes a derivative with respect to ϕ The boundary conditions for the bounce:

$$\lim_{\tau\to\pm\infty} \phi(\tau, \vec{x}) = \phi^- \tag{2.20}$$

and

$$\frac{\partial\phi}{\partial\tau}(0, \vec{x}) = 0 \tag{2.21}$$

The coefficient B is

$$B = S_E = \int d\tau d^3x [\frac{1}{2}(\frac{\partial\vec{\phi}}{\partial\tau})^2 + \frac{1}{2}(\nabla^2\phi)^2 + V] \tag{2.22}$$

For B to be finite it is necessary that

$$\lim_{|\vec{x}|\to\pm\infty} \phi(\tau, x) = \phi^+ \tag{2.23}$$

This is consistent with the description of vacuum decay in our introduction: quantum fluctuations will nucleate a bubble somewhere in space; far from this place, the false vacuum will be undisturbed. No non-trivial solution of these equations

is invariant under spatial translations; any spatial translation of a solution is also a solution, with the same Euclidean action. To obtain the total width of the false vacuum, we must integrate over the group of spatial translations, as mentioned at the end of the previous section. We can guess the form of the solution of these equations; they are all consistent with the assumption that is invariant under 4D Euclidean rotations.

If we define ρ by

$$\rho = (\tau^2 + |\vec{x}|^2)^{\frac{1}{2}} \tag{2.24}$$

then the assumption is that ϕ is a function of ρ only

With this, (2.19) becomes

$$\frac{d^2\phi}{d\rho} + \frac{3}{\rho}\frac{d\phi}{d\rho} = V'(\phi) \tag{2.25}$$

Eq (2.20) and (2.23) become

$$\lim_{\phi\to\infty} \phi(\rho) = \phi^+ \tag{2.26}$$

Eq (2.22) becomes

$$B = S_E = 2\pi^2 \int_0^\infty \rho^3 d\rho (\frac{1}{2}(\frac{d\phi}{d\rho})^2 + V) \tag{2.27}$$

and

$$\frac{d\phi}{d\rho}\Big|_0 = 0 \tag{2.28}$$

Coleman (1977) in his initial development of the false vacuum theory believed that using Eqs. (2.25)-(2.28) it could be shown that they always have a solution; that the system would always admit an O(4)-invariant bounce; we will demonstrate that here, although in the next chapter we will find a special case in which this is not true. If we represent ϕ to as a particle and ρ as time, then (2.27) represents the equation for a particle moving in an upside down (or -V) potential [Figure 2.2],

with a viscous damping force with Stoke's law coefficient inversely proportional to time . Using (2.28) we release the particle from rest at time $\rho = 0$. If we choose our initial position carefully, when we release the particle from rest, it will travel down our potential and come to rest at precisely the top of the hill ϕ^+ in Fig., at ρ infinity. We can demonstrate what is known as the overshoot/undershoot argument: if we release ϕ from a position sufficiently close to the left of ϕ_-, it will undershoot its final rest atop ϕ^+. If the particle does not have enough energy when released, it simply won't have enough energy as with a classical analog of a ball rolling down a hill with some momentum (and then back up a hill). There is always a friction force present but it does not come into play if the particle doesn't have enough energy to begin with. If we release it slightly to the right of ϕ_-, it will overshoot ϕ^+. Following this logic there must be an initial release point between the two such that the particle comes to a halt atop ϕ^+ at ρ infinity. If we choose ϕ to be initially sufficiently close to ϕ_-, we can arrange that it stays arbitrarily close to ϕ_- for arbitrarily large ρ. But for sufficiently large ρ, the viscous damping force can be neglected, since its coefficient is inversely proportional to ρ. If we neglect the viscous damping, however, the particle overshoots.

2.3 Thin-Wall Approximation

Let's consider a symmetric function of ϕ, $V_{sym}(\phi)$

$$V_{sym}(\phi) = V_{sym}(-\phi) \tag{2.29}$$

with minima

$$V'_{sym}(\pm r) = 0 \tag{2.30}$$

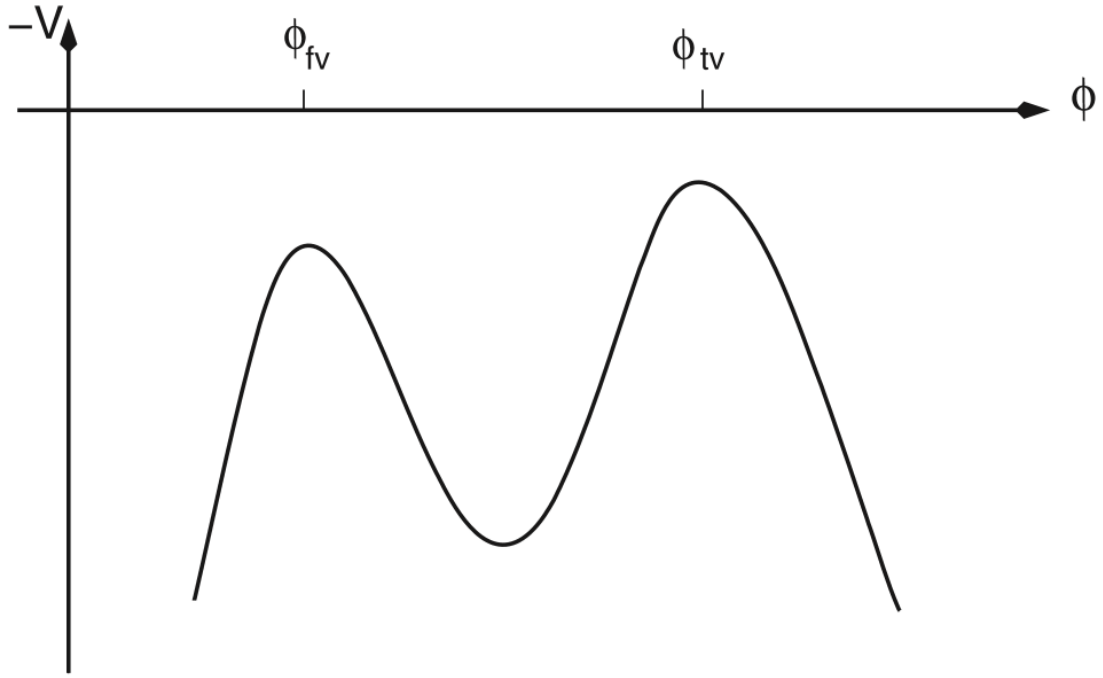

Figure 2.2: The "undershoot-overshoot" upside down potential. The field is released at $\rho = 0$ from a point arbitrarily close to the true vacuum maximum and must come to rest at the false vacuum.

Let's define

$$\mu^2 \equiv V''_{sym}(\pm r) = 0 \tag{2.31}$$

we will add a small symmetry breaking term to V_{sym}

$$V = V_{sym} + \frac{\delta}{2r}(\phi - r) \tag{2.32}$$

where δ represents the energy difference between the true and false vacua. In the limit of small δ it is possible to compute B. We must choose our initial field ϕ to be very close to ϕ_- such that it won't lose too much energy to damping. The field will stay close to ϕ_- until a very long time $\rho = R$. Near R, the field will move rapidly through the trough and then proceed up the hill, slowly towards its rest atop ϕ^+. This 1D particle is analogous to a 4D spherical bubble of radius R, with a thin wall separating the false vacuum from the true vacuum within the bubble region. We need more information about the bubble wall. For δ near R, we can neglect the viscous damping term of (2.25), and also the δ-dependent term in V_{sym}. This gives the equation for a soliton in a 1D field theory

$$\frac{d^2\phi}{dx^2} = V'_{sym}(\phi) \tag{2.33}$$

with x being the spatial coordinate in 1D. The fundamental solution is an odd function of x, $\phi_1(x)$, defined by

$$x = \int_0^{\phi_1} \frac{d\phi}{\sqrt{2V_{sym}(\phi)}} \tag{2.34}$$

The 1D action of this solution is

$$S_1 = \int dx[\frac{1}{2}(\frac{d\phi_1}{dx})^2 + V_{sym}] = \int_{-r}^{r} d\phi\sqrt{2V(\phi)} \tag{2.35}$$

For $|x| >> 1$

$$\phi_1 = [\pm r - Ke^{-\mu|x|}] \tag{2.36}$$

where K is a constant that depends on the form of U. We can express analytically our expression of the bounce in terms of ϕ_1

$$\begin{aligned} \phi &= -r, \rho << R \\ &= \phi_1(\rho \approx R) \\ &= r, \rho >> R \end{aligned} \tag{2.37}$$

We just need the value of R for our thin wall description. The action of this 4D bubble is

$$S_E(R) = 2\pi^2 R^3 S_1 - \frac{1}{2}\pi^2 R^4 \delta \tag{2.38}$$

The first term in (2.38) comes from the wall and can be viewed as a surface tension, the second term from the interior of the bubble. Taking the derivative of this

$$\frac{dS}{dR} = 6\pi^2 R^2 S_1 - 2\pi^2 R^2 \delta \tag{2.39}$$

Solving this,

$$R = \frac{3s_1}{\delta} \tag{2.40}$$

We can use this to compute B

$$B = S = \frac{27\pi^2 S_1^4}{2\delta^3} \tag{2.41}$$

This is the expression for B in the limit of small δ

Chapter 3: Fubini Bounce

3.1 Unstable Quartic Potential

As established in the previous section, due to the undershoot/overshoot method and due to the continuity between the extreme cases it is a guarantee that there must exist a bounce solution which lands ϕ_0 at ϕ^+ with zero velocity, corresponding precisely to the bounce solution. However there are potentials for which this isn't the entire picture. One well known example is the unstable quartic potential $-\frac{\lambda}{4}\phi^4$ (which is relevant in studying the stability of the Standard Model Higgs potential). This potential has the property that solutions of the Euler-Lagrange eqs (2.25) with an arbitrary starting point are all bounces, as they reach ϕ^+ at $\rho \to \infty$. These are known as "Fubini bounces"[5] and can be obtained analytically

$$\phi_B(\rho) = \frac{\phi_0}{1 + \frac{\rho^2}{R^2}} \tag{3.1}$$

with

$$\frac{1}{R^2} = \frac{1}{8}\lambda\phi_0^2 \tag{3.2}$$

This gives the tunneling action

$$S_E(\phi_B) = \frac{8\pi^2}{3\lambda} \tag{3.3}$$

There is no singular ϕ_0 bounce solution because the potential is scale-invariant; this leads to a degenerate family of instantons with arbitrary ϕ_0 and size $R \sim \frac{1}{\phi_0}$ and is why the tunneling action doesn't depend on ϕ_0 . The action S_E has a flat direction in field configuration space, consisting of Fubini bounces, with the value given in (3.2). Scale invariance of this potential implies that, if $\phi_B(\rho)$ is a bounce solution, then the rescaled $r\phi_B(r\rho)$ with $(r > 0)$ is also a bounce solution. This amounts to a rescaling

of $\phi_0 \to r\phi_0$, or, rescaling the bounce radius R $\to$ R/r. There exist other potentials with FV for which there is no Euclidean bounce solution. Consider as an example the class of potentials with a false vacuum at $\phi^+ = 0$, with a barrier that reaches its maximum at $\phi_T > 0$, beyond which the potential is $V(\phi > \phi_T) = -\lambda\frac{(\phi-\phi_T)^4}{4}$. Due to the special properties of the unstable quartic potential, any solution of equation (2.25) starting at $\rho = 0$ with some field $\phi_0 = \phi_0 > \phi_T$ and $\phi(0) = 0$ ends at $\phi(\infty) = \phi_T$, never reaching ϕ^+. Thus this class of potentials has no bounce.

Another example of this bounce-less potential is

$$V(\phi) = \frac{1}{2}m^2\phi^2 - \frac{\lambda}{4}\phi^4 \tag{3.4}$$

This is seen as follows: Assume there is a bounce $\phi_B(\rho)$ and consider the rescaled field profile $\phi r(\rho) \equiv r\phi_B(r\rho)$. After changing the integration variable, the Euclidean action for the rescaled field reads:

$$S_E[\phi_r] = 2\pi^2 \int_0^\infty [\frac{1}{2}(\frac{d\phi_B}{d\rho})^2 - \frac{1}{4}\lambda\phi_B^4]\rho^3 d\rho + \frac{2\pi^2}{r^2}\int_0^\infty [\frac{1}{2}m^2\phi_B^2]\rho^3 d\rho \tag{3.5}$$

Since $\phi_B(\rho)$ extremizes the Euclidean action, therefore, one should have $\frac{dS_E[\phi_r]}{dr} = 0$ at r = 1, which for $m^2 \neq 0$ gives the condition

$$\int_0^\infty \phi_B^2\rho^3 d\rho = 0 \tag{3.6}$$

which can only be satisfied for $\phi_B(\rho) \equiv 0$. This contradicts the initial assumption about the existence of a non-trivial bounce. Espinosa developed a few different treatments of 'pseudo-bounces', for potentials without a bounce. He first does it by revisiting the problem within the standard Euclidean formalism to find pseudo-bounce profiles with a finite action value that can reconcile vacuum decay; he uses the generic profile of the scale-invariant potential $V = -\frac{\lambda}{4}\phi^4$. Also discussed is the Minkowskian

WKB approach which is used to validate Coleman's Euclidean bounce solution, as well as a different formalism, introducing a tunneling potential V_t to calculate actions without Euclidean bounces. This new approach introduces V_t to describe the decay process and formulates the action calculation as a simple variational problem in field space. However, let's focus on the standard Euclidean formulation of the pseudo-bounce, then later we can compare this approach to our own numerical calculation of a modified version of this class of potential.

3.2 Euclidean Pseudo-Bounce

For our convenience we will start (following Espinosa closely) with the simple quartic potential $V = -\frac{\lambda}{4}\phi^4$. We modify this V so that there is a false minimum at some $\phi^+ < 0$ and a deeper true minimum at $\phi^- > -\phi^+$ without changing the potential between ϕ^+ and ϕ^-, [Figure 3.1]. We then consider the decay $\phi^+ \to \phi^-$, which gives the simplest no-bounce potential. So we calculate $S_E(\phi^+ \to \phi^-)$and see how it varies with increasing ϕ^- and fixed ϕ^+. Our chosen scale-invariant potential allows us to guess some key properties of $S_E(\phi^+ \to \phi^-)$; The only mass scales in the problem are ϕ^+ and ϕ^- ; therefore, the dimensionless tunneling action ($\hbar = 1$) must be a function of their ratio:

$$S_E(\phi^+ \to \phi^-) = f(-\phi^+/\phi^-) \tag{3.7}$$

The ratio $(\frac{-\phi^+}{\phi^-})$ is in the interval (0, 1) and the two boundary values of this interval are simple. For $\phi^- \to -\phi^+$, these vacua become degenerate and the decay rate vanishes. This implies that

$$f(1) = \infty \tag{3.8}$$

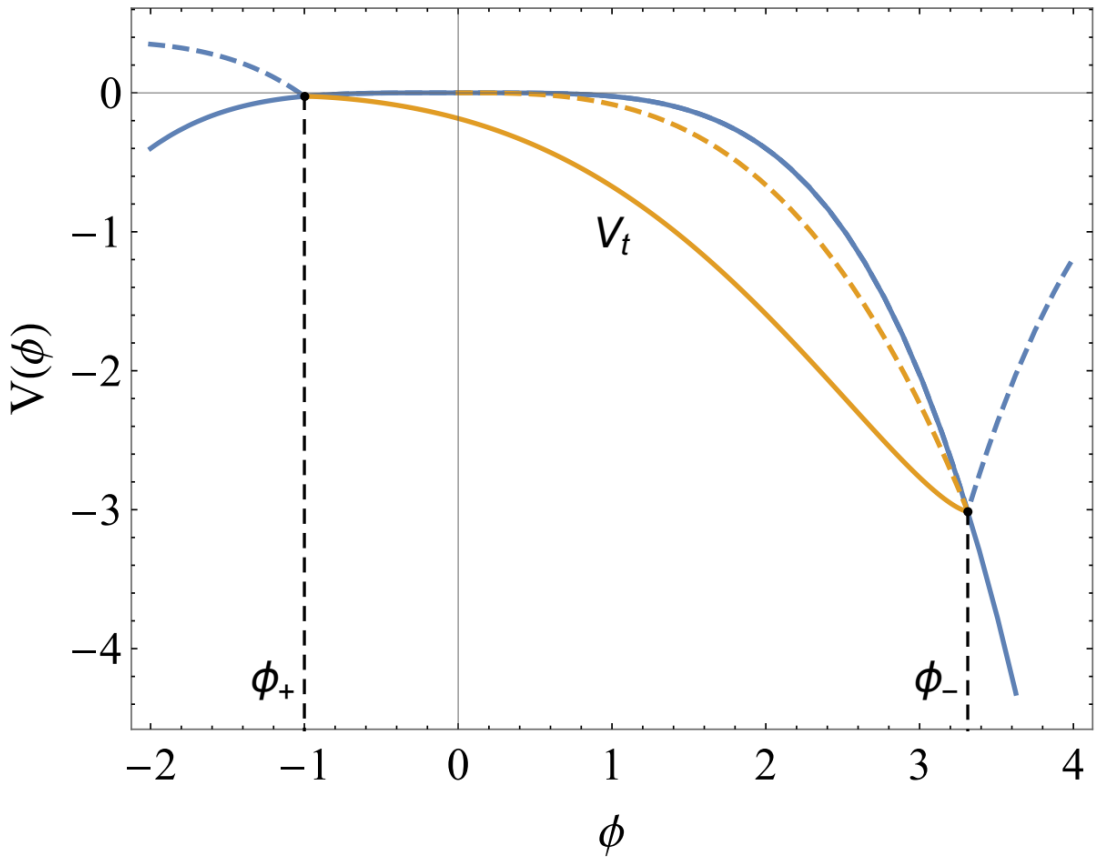

Figure 3.1: Figure 3.1: Potential $V(\phi) = -\lambda\frac{\phi^4}{4}$ (blue lines) for $\lambda = 0.1$. Tunneling from ϕ^+ to ϕ^- can be studied by modifying the potential as shown by the dashed lines (that create minima at $\phi^{\pm}$). The corresponding restricted tunneling potential, V_t , for such decay is also plotted. The dashed line corresponds to the standard V_t that fails to reach ϕ^+, as in Fig. 1

The approach to this limit is described, as we recall from chapter 2, by our thin-wall approximation

$$S_{E(thin-wall)} = \frac{27\pi^2 S_1^4}{2\delta^3} \tag{3.9}$$

and wall tension

$$\sigma_{wall} = \int dx[\frac{1}{2}(\frac{d\phi_1}{dx}^2) + V(\phi) - V_{FV}] = \int_{-r}^{r} d\phi\sqrt{2(V(\phi) - V_{FV}} \tag{3.10}$$

where $r\pm = \phi^{\pm}$ and

$$\sigma_{wall} \cong \frac{4}{3}\sqrt{\frac{\lambda}{2}}(-1)(\phi_-^3), (\phi^{\pm} = \phi_{\pm}) \tag{3.11}$$

where $K(-k^2)$ is the complete elliptic integral of the first kind [4]

$$K(-k^2) = \int_0^{\pi/2} \frac{1}{\sqrt{1 + k^2 \sin^2\theta}} d\theta \tag{3.12}$$

and just to differentiate between V and U (although serving the same purpose)

$$\epsilon = V(\phi_+) - V(\phi_-) = \lambda\frac{(\phi_-^4 - \phi_+^4)}{4} \tag{3.13}$$

which is the energy difference between the vacua. For $\phi_+ = 0$ and arbitrary ϕ_- we recover our Fubini bounces and (3.2)

$$f(0) = \frac{8\phi^2}{3\lambda} \tag{3.14}$$

We should asymptotically reach the same limit for $\phi_+ \neq 0$ and $\phi_- \to \infty$. This limit (with no bounce for V) will also be reached from above, with f being a monotonically decreasing function with $(-\phi_+/\phi_-) \to 0$. We can explicitly confirm these expectations by obtaining bounce solutions after enforcing minima at $\phi_\pm$. These minima allow $\phi(\rho)$ to wait at ϕ_- and start rolling only after some time ρ_-; [Figure 3.2]. This starts the

particle off with reduced friction, making it possible to reach ϕ_+ with zero velocity at some finite ρ_+. The analytical solution to this field value from Espinosa is

$$\phi(\rho) = \begin{cases} \phi_- & \text{for} \quad \rho < \rho_- \\ \frac{\rho_\phi}{\rho} k^{1/2} sn[sn^{-1}[k^{-1/2}, k^2] + \frac{log(\rho/\rho_-)}{\sqrt{k^2-1}}, k^2] & \text{for} \quad \rho_- < \rho < \rho_+ \\ \phi_+ & \text{for} \quad \rho > \rho_+ \end{cases}$$

with $sn(z, -k^2)$ being the Jacobi Elliptic sine function, with

$$k^2 \equiv \frac{\sqrt{1 + \lambda^2 \rho_\phi^4} + 1}{\sqrt{1 + \lambda^2 \rho_\phi^4} - 1} \tag{3.15}$$

and

$$\rho_\phi \equiv \rho_- \phi_- = -\rho_+ \phi_+ \tag{3.16}$$

which leads to this relation ($\frac{\rho_-}{\rho_+} = \frac{-\phi_+}{\phi_-}$). To complete our solution we find a relation between ρ_-/ρ_+ and ρ_ϕ, which we obtained by requiring $\phi(\rho_+) = \phi_+$. Using the periodicity properties of sn [in particular $sn(x + 2K(-k^2), -k^2) = -sn(x, -k^2)$], we get

$$\frac{\rho_-}{\rho_+} = \exp\left[2K(-k^2)\sqrt{k^2 - 1}\right] \tag{3.17}$$

This is shown in [Fig 3.3]. The field profile of (3.12) would be a standard Euclidean bounce if it had a true minimum in ϕ_-, which is why it is named "pseudo-bounce". This class of potentials is special because the action $S_E(\phi_+ \to \phi_-)$ is a monotonically decreasing function of ϕ_- with the smallest value reached asymptotically as $\phi_- \to \infty$. The minimum of the action is pushed away to infinity: this is why there is no bounce. In other words, $\phi_+ \neq 0$ breaks the scale invariance and lifts the flat direction of Fubini bounces into a valley of configuration space. We can still

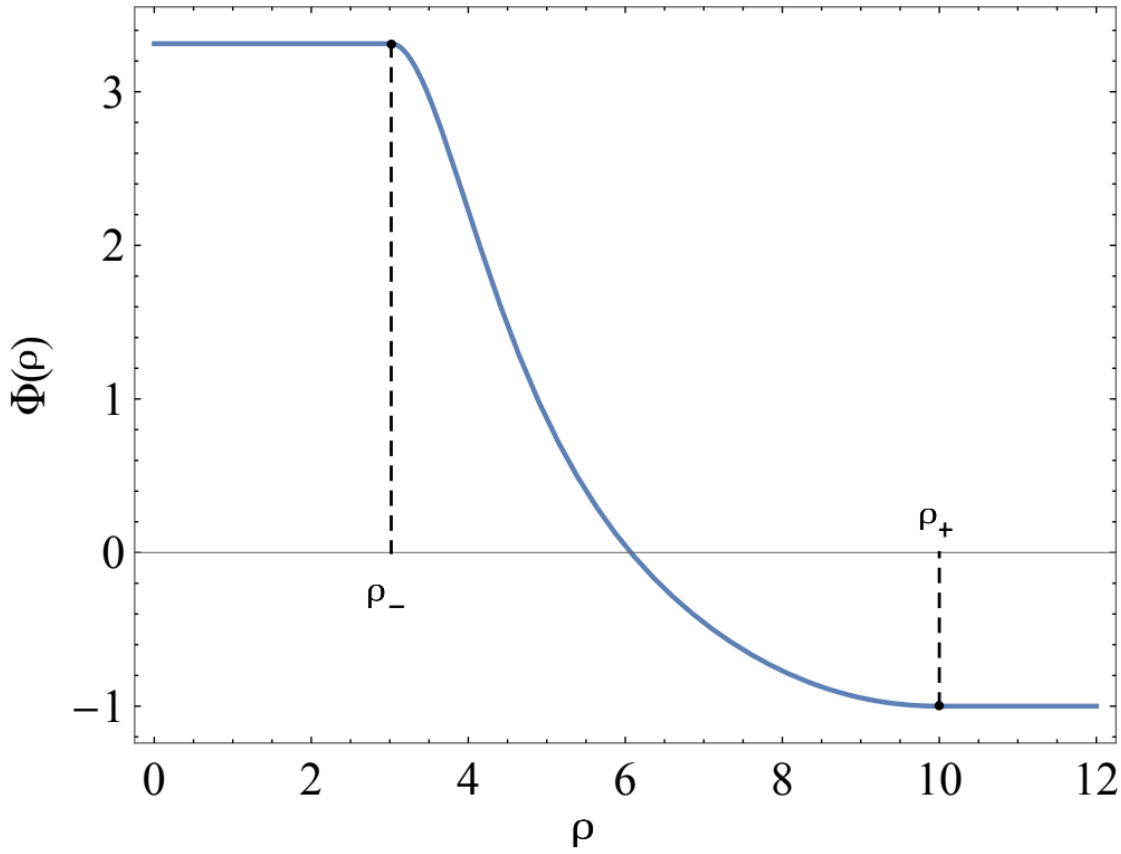

Figure 3.2: Profile of the Euclidean pseudo-bounce for the potential of Fig. 3.1 as given by Eq. (3.15), with $\phi^+ =$ - 1 and $\rho^+ = 10$

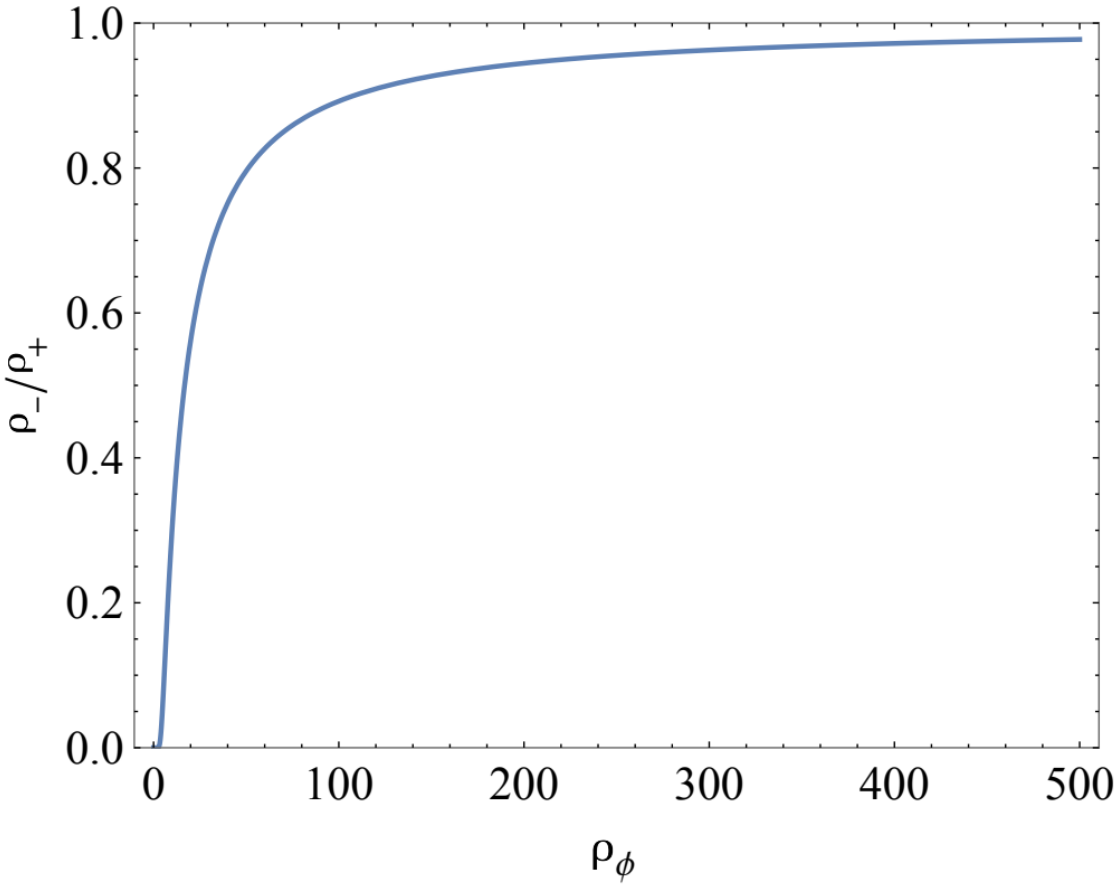

Figure 3.3: The ratio ρ/ρ^+ as a function of $\rho_\phi = -\rho^+\phi^+ = \rho^-\phi^-$

use ϕ_- as a parameter along the bottom of this valley. The action along it decreases towards the scale-invariant value, achieved only asymptotically, when the scale breaking parameter $(-\phi_+/\phi_-) \to 0$. This shows that the decay of the ϕ_+ false vacuum is dominated by small instantons and therefore is sensitive to ultraviolet (UV) effects that might modify the potential at large field values. Renormalization effects also may modify the shape of the valley bottom. Espinosa (2019).

Chapter 4: Numerical Methods

4.1 A comparison using a deformed $\lambda\phi^4$ potential

In this section, we compare Espinosa's pseudo-bounce calculation of the bounce to a numerical method using a deformed potential. Specifically, we want to deform a $-\lambda\phi^4$ potential such that it now has a true and false vacuum. We will evaluate the bounce action as we move the true vacuum away from the false vacuum while keeping a median region where the shape of the potential overlaps with our unstable $\lambda\phi^4$ potential. We also want to keep the false vacuum as close as possible to zero since zero is essentially the false vacuum of $-\lambda\phi^4$. The motivation for this approximation is that potentials are expected to be bounded from below. The problematic $-\lambda\phi^4$ potential could only be an approximation of the potential for small ϕ values.

We know that for these deformed potentials there is going to be a solution; because there is a true vacuum the overshoot/undershoot method will always work. The problematic potentials as discussed previously do not have a true vacuum, so the overshoot/undershoot method does not work. When we calculate the decay of the false vacuum using the Euclidean bounce method we expect a thin wall solution when the potential difference between the true vacuum and false vacuum is small. The Euclidean equation of motion has a time-dependent friction term, which will be become negligible after a long time. If the initial field ϕ will be released from some point offset from the true vacuum, the negligible friction will guarantee the field can reach the false vacuum. Or if the potential is not high enough the field won't have the energy to make the false vacuum. But for the $\lambda\phi^4$ potential you cannot make adjustments for either of these, the friction term will rise proportionately.

In these potentials where the difference between the false and true vacuum is large, the thin wall approximation will not work; we have a thick wall. In the thin wall scheme, the decay of the vacuum nucleates a bubble; the inside region of the bubble is true vacuum and outside of the bubble is false vacuum. In the case of a thick wall there is no well defined true vacuum region; the value of the field at the center is a medium between the true and false vacuum which gradually transitions outside of the bubble region into the false vacuum. For the thick wall the value of the field at the center is well-defined given a particular potential, while for the Fubini instanton this is not the case. The Fubini instanton interpolates any value at the center and the false vacuum at infinity. All the solutions have the same action. So we know that for a $\lambda\phi^4$ potential there is no extreme bounce solution. By comparing with the deformed potential the question we have to ask is, where does this break down?

Let's take some generic potential which is modified from this: $(-\lambda\phi^4 + \alpha\phi^5 + \beta\phi^6)$ This potential is a double-well shape, with its true vacuum at some lower energy than the false vacuum. This potential has such features that it skims along the $\lambda\phi^4$ shape in an intermediate range between two points of intersection; it contains both a false and true vacuum and thus it has bounce solutions corresponding to a true vacuum but in the intermediate region shares the same bounceless behavior as the first potential. So we want to know what happens up until the point of intersection, where the 'standard' unstable quartic potential breaks down? What happens as the true vacuum from our modified potential asymptotically approaches the region of overlap for $\lambda\phi^4$

We do this numerically. Using Mathematica, we first define our potentials, V_{one} and V_{two}; the former corresponding to $-\lambda\phi^4$ and the latter, to our modified potential

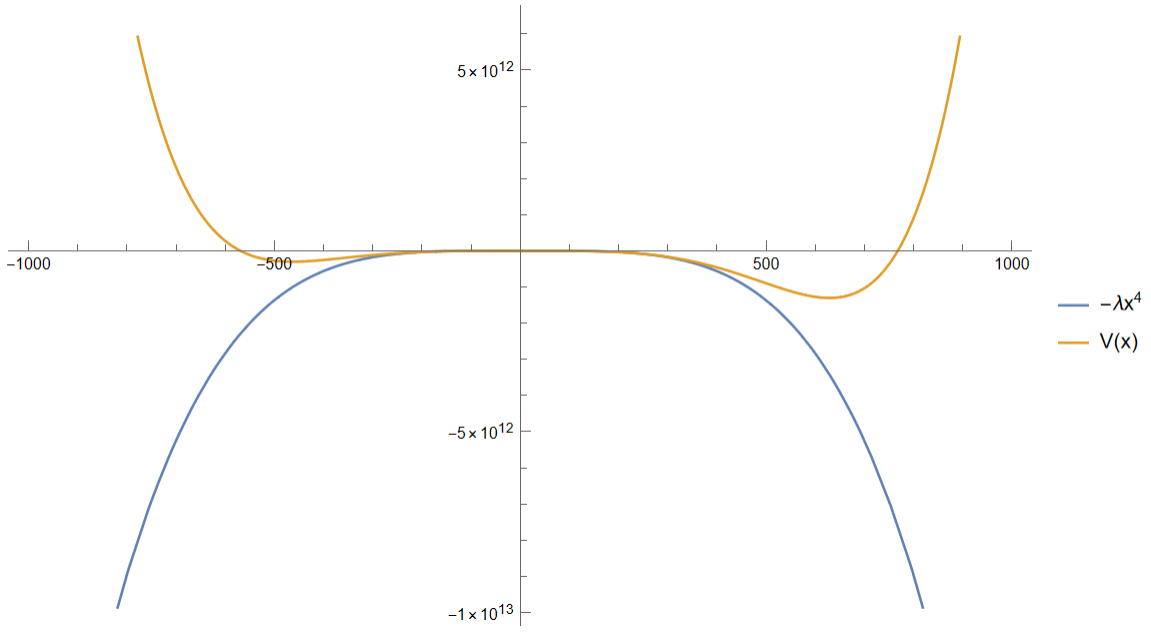

Figure 4.1: The value of the potentials V_{two} and V_{one} at ϕ versus the value of ϕ.

$V(\phi) = -\lambda\phi^4 + \alpha\phi^5 + \beta\phi^6$. A plot of these two potentials is shown in [Figure 4.1]. α and β are constants which we choose to fit V_{two} to V_{one}, such that they overlap in the intermediate bounceless region of V_{one} but still create both false and true vacuum minima in the adjacent regions. We wanted to keep the shape of V_{two} in the overlap region as close as possible to maintain the same behavior but by choosing different combinations of α, β, and λ and varying them individually for multiple iterations, we could find where the true vacuum of V_{two} asymptotically approaches V_{one}. To choose our initial ϕ, we wanted to use the same undershoot/overshoot method with an upside down potential, starting very near the true vacuum (which would be at the top of the first hill) so that it has the field velocity necessary to come to rest just at the top of the false vacuum hill. Choosing the initial ϕ for this requires choosing a position with a precision of 15 or more digits to find the exact bounce. The differential equation

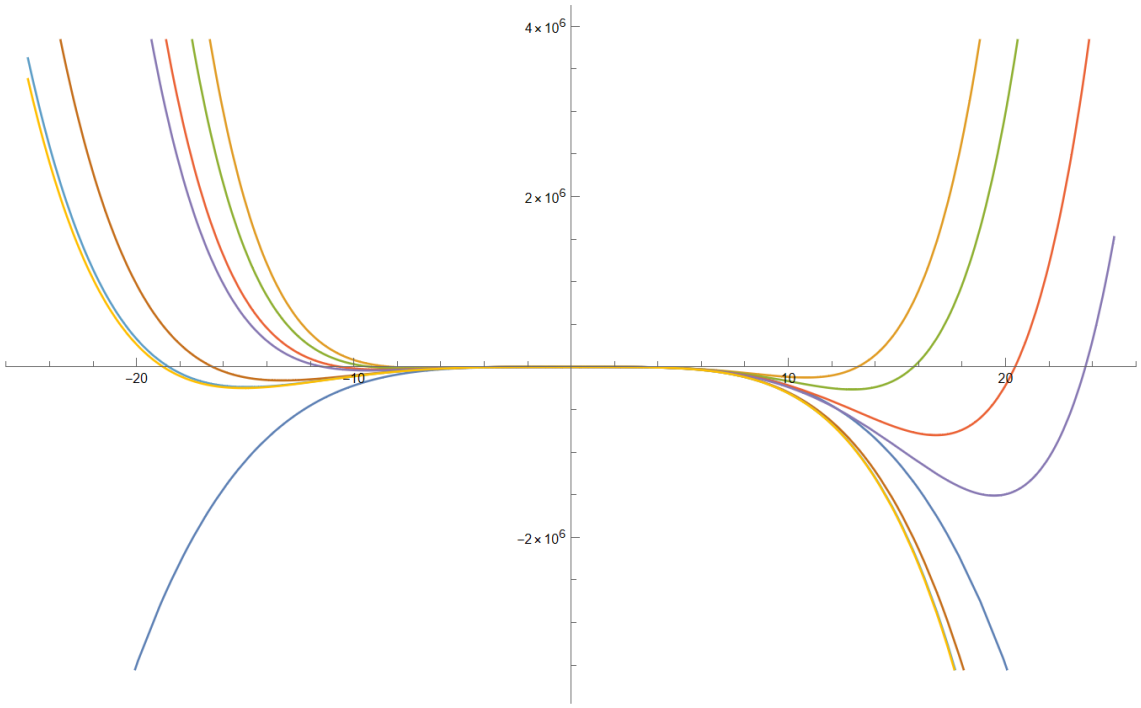

Figure 4.2: A plot of V_{three}, an overlay of multiple V_{two} curves; These are for a range of values of α, β, and λ given in table 1.

used (in mathematica) was

$$x''(t) = -\frac{3}{t}x'(t) - 4\lambda(x)^3 + 5\alpha x(t)^4 + \beta 6x(t)^5 \tag{4.1}$$

Here x(t) = $\phi(\rho)$. The initial conditions of our equation of motion were $x(\epsilon)$, the initial ϕ which is arbitrarily close to the TV value based on the chosen α, β, and λ; also $x'(\epsilon) = 0$ since ϕ starts with zero velocity. ϵ is = 1/500000 to account for the $-3/t$ term in Eq 4.1

The best fits we were able to produce were with values for λ held constant but varying α and β; this maintained the overall shape and closeness of V_{two}, to V_{one}. An example of this with λ and α held constant, but varying β is shown in [Figure 4.2]. The values for ϕ are very large compared to α and β. We generated a table of values

for α, β, and ϕ corresponding to solutions of equations of motion; the bounce action was calculated numerically. We input table values into an integral for B, which is just the difference between the action integrals S_{bounce} to S_{FV}. Both the action for the numerical and the Espinosa solutions approaches zero as the true vacuum moves to infinity. The Espinosa solution always produce a negative number while our numerical values are positive but approach zero as β decreases. This indicates that our approximation becomes less reliable as we move from thin to thick wall profiles. The semiclassical bounce approximation is not to be trusted when the decay rate is of order one. The numerical result is not bounded from below by the action of the Fubini instanton, which was the original expectation because the deformed potential is very different from $-\lambda\phi^4$ as the true vacuum moves to infinity. It would be interesting to see if this behavior persists for more sophisticated deformations of the potential.

Comparing the ratio of FV V(x) to the solution of our equation of motion [Figure 4.3], we created a bounce solution profile; in this we can see how the bubble wall thickness changes with the range of initial field values and find the limit of when the bounce solution no longer is a bounce. When the solutions are thin wall, the FV section of the profile is broader, as well as the intersection between FV V(x) and TV V(x). There are a range of FV and TV V(x) values for which there are no longer bounce solutions; the flat part will shrink to a thick wall profile, and the TV will no longer reach the range of bounce solutions (the blue line of figure 4.4). The solution profile for table 1 varies as such: The first few solutions correspond to that of a thin wall. As our initial ϕ increases, the difference between FV-TV also increases. For a thin wall case this difference remains relatively small, i.e the value of the potential between the two regions corresponds to a well-defined bubble. Our initial ϕ should get further and further away from our TV value, it is being released further away;

B	β	ϕ_{fv}	$\phi(0)$	ϕ_{tv}	$V(\phi_{\text{tv}})$	$V(\phi_{\text{fv}}) - V(\phi_{\text{tv}})$
35.1992	.201	-6.6967	10.822	10.8219	-124510	112096
23.0682	.151	-7.4528	12.944	12.9439	-264710	246053.1
12.7577	.101	-8.5867	16.795	16.7963	-801355	769501.6
9.2409	.081	-9.2355	19.468	19.4721	-1.51133×10^6	1469484.6
3.3310	.040	-11.3516	32.012	32.0807	-1.33495×10^7	13259821.8
1.2829	.020	-13.3007	54.245	54.759	-1.47136×10^8	146977087
0.5448	.010	-14.8929	95.345	97.8096	-2.15108×10^9	2150843198
0.4630	.009	-15.0947	104.188	107.224	-3.31311×10^9	3312873198
0.2257	.005	-16.0202	173.134	181.854	-4.09479×10^{10}	40947595253
0.1881	.004	-16.288	211.097	223.58	-1.10847×10^{11}	$1.10846677485 \times 10^{11}$
0.1139	.003	-16.574	273.674	292.963	-4.11529×10^{11}	$4.11528657812 \times 10^{11}$
0.1083	.002	-16.8805	397.310	431.464	-2.73208×10^{12}	$2.732079635912 \times 10^{12}$
0.0335	.001	-17.2106	760.908	846.377	-7.5764×10^{13}	$7.5763999611390 \times 10^{13}$

Table 4.1: Tabulated values for the constants and ϕ on which our modified potential depends, for our numerical calculation. The B values approach zero with β. This is the case which displays thick wall solution profiles, with λ and α held constant (with values of 21.85 and -0.995 respectively) and varying β; this was also done for the same potential, with varying α and β and constant λ in Table 2. Table 2 only produced thin wall solutions, while Table 1 saw a progression towards thick walls as β decreased.

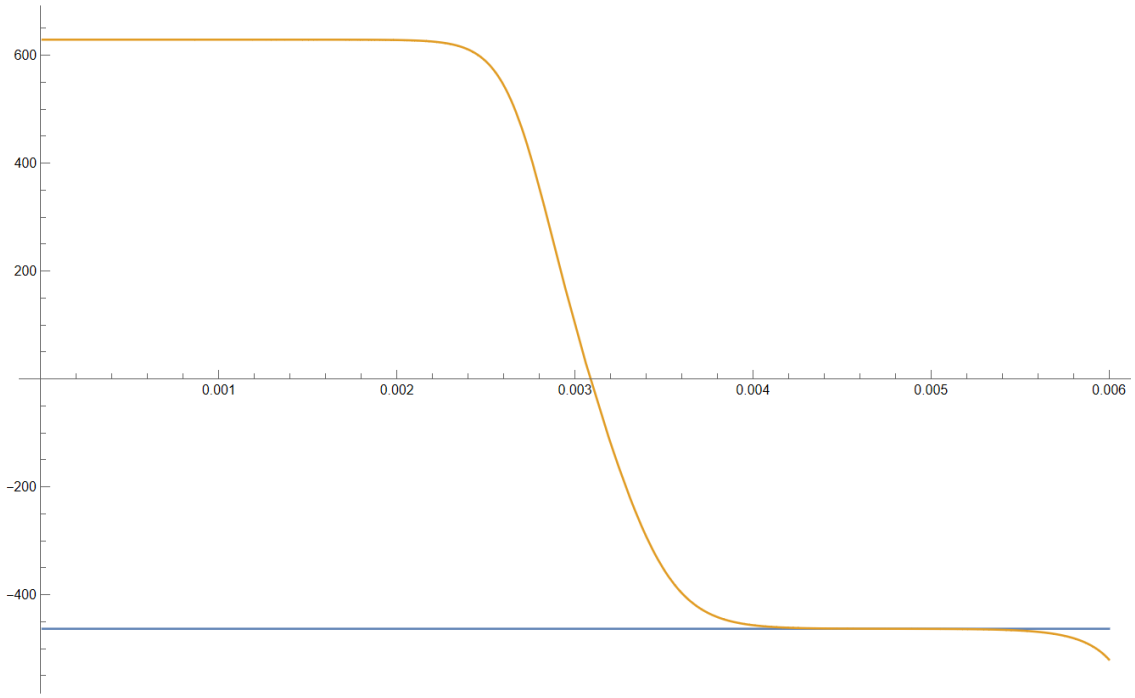

Figure 4.3: The solutions of the equations of motion for V_{two} and the false vacuum minima over a time interval. At the start of the interval the field (orange line) is in the true vacuum, represented by the upper flat portion of the curve. As the field rolls away from the true vacuum state it comes to rest atop the false vacuum minima (blue line).

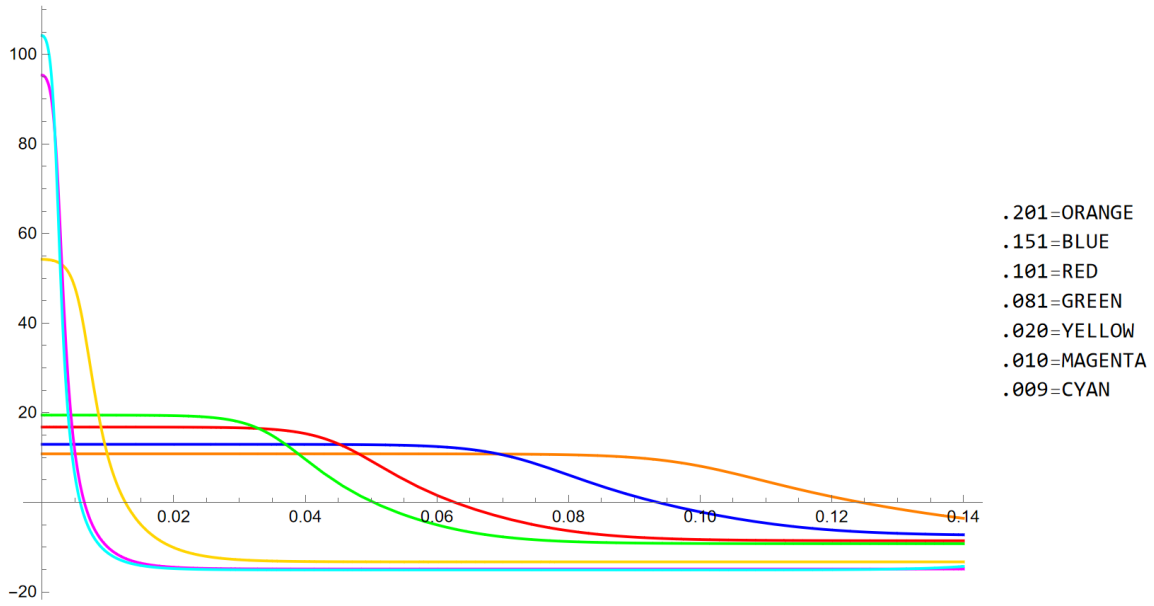

Figure 4.4: The change in wall thickness in descending order, chosen for 7 values of β. The cyan, magenta and yellow lines correspond to thick wall solutions, while the remaining are thin walls.

this also further offset the field value for FV; (perhaps there is a V with solutions for which the FV field could be stationed at the origin and the TV could vary). The field will have less time to slow roll and gather friction. The TV value is the exit point of the field after tunneling from the FV. As our values for initial ϕ in table 1 increase, we should approach a "thick wall" profile. In the multi-colored plot [Figure 4.4] we can see that the first few lines correspond to a 'flat' profile, which are thin wall solutions. The last few lines are thick walls, there is barely any flat region which means there is no TV bubble, just a gradual change from one false vacuum minima to the next minima. A similar plot is done for figures 4.5-4.6, comparing ϕ values for our numerical calculation against those done analytically by Espinosa (2019) and Fubini (1976). We've selected 4 values of beta each for comparison. To find the Espinosa solutions $\phi(\rho)$, we started with the TV and FV phi values from our V, plugging these

into eq. (3.17) but multiplied by a factor of ρ_+, to solve for k. Plotting the intersection between this function and ϕ_-, we can find where k is expected to be, or by finding the root of this equation. Once we find k we need to find ρ_ϕ; we simply take the square root of eq (3.15) and as before plot against the intersection of our k value. Alternatively, by finding the root of this equation. Once we have ρ_ϕ we use (3.16) to find ρ_- and ρ_+. The exact values for Espinosa $\phi(\rho)$ appear to be discontinuous at fvphi and tvphi, with the slope approaching zero at both points. In Figure 4.5-4.6, the Espinosa solutions seem to have a more well defined true vacuum flat region. This remains the case as our B values change. Also the field in this case is strictly starting from the TV compared to the numerical case which is offset by an increasing amount as beta decreases. There is a small bubble region which transitions to a false vacuum, while the numerical solutions don't have a bubble but some minima which gradually transitions to an ill-defined lower minima. The Fubini solutions (which see their FV approach zero) remain without a well-defined TV as beta changes. It also has a broader slope than Espinosa or the numerical solutions, approaching its FV more slowly. For these it is difficult to know what happens in the TV, since the action is not dependent on the value of the field inside the bubble. If the minimal action is preferred by nature then we have yet to understand what happens as the TV of the modified potential approaches $\lambda\phi^4$. The profile of the numerical solutions seem to better approximate Espinosa with decreasing values of β, at least in the case of the values given in Table 1 but as the values of ϕ go to infinity this is unclear. In this analysis our results were obtained by a potential with α, β and λ constant values chosen in such a way that the FV was slightly offset at the values decreased; it moved increasingly slight to the left of the origin. There may be a potential which exists in which the FV could be stationary at the origin as the values of our constant change;

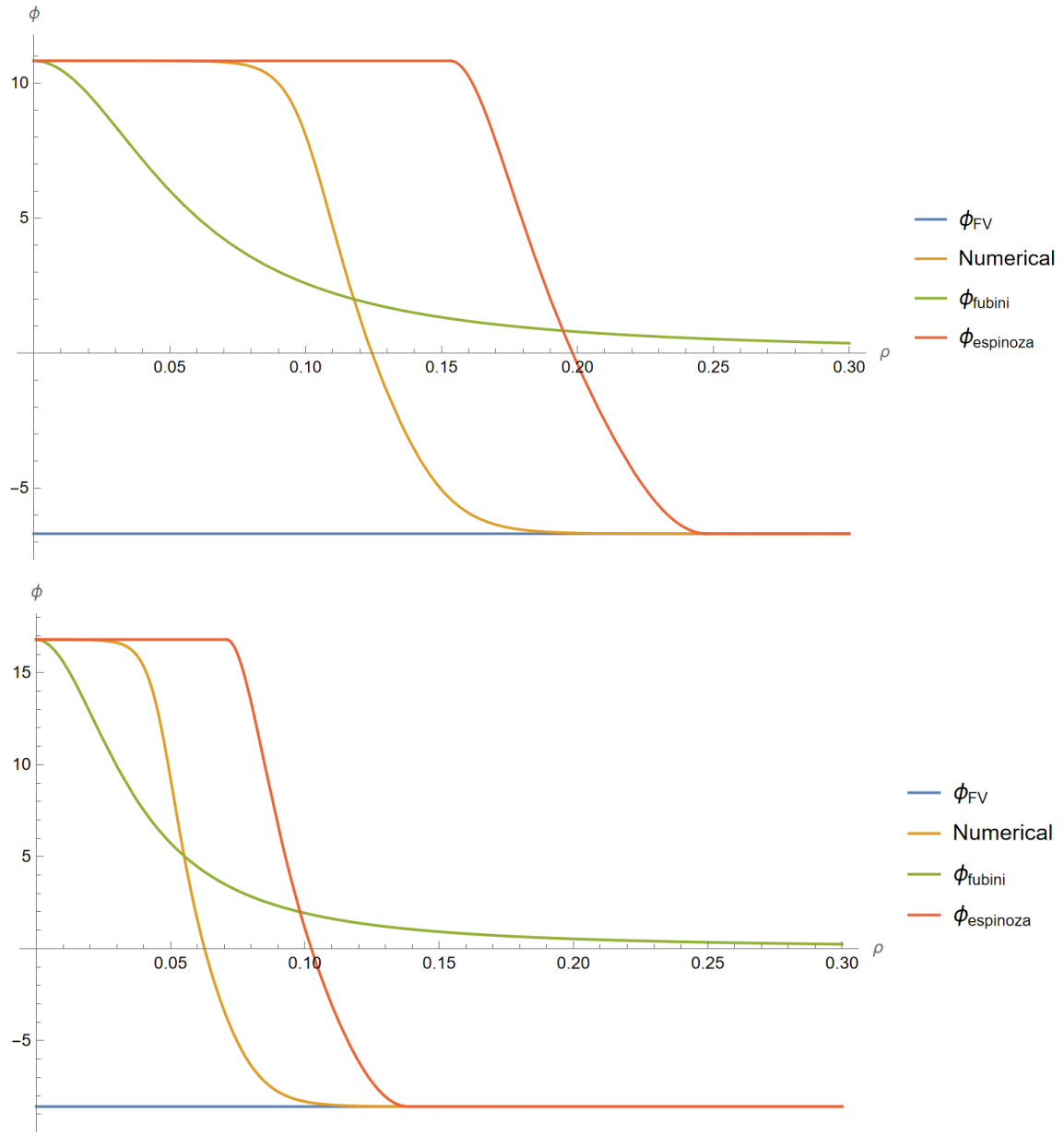

Figure 4.5: A comparison of several $\phi(\rho)$ profiles: those of Fubini, Espinosa, and our numerical solutions as they decay to ϕ_{FV}, with four snapshots as our ϕ_{TV} goes to ∞.

what effect this would have on our solution profiles might make this a worthwhile exploration in the future.

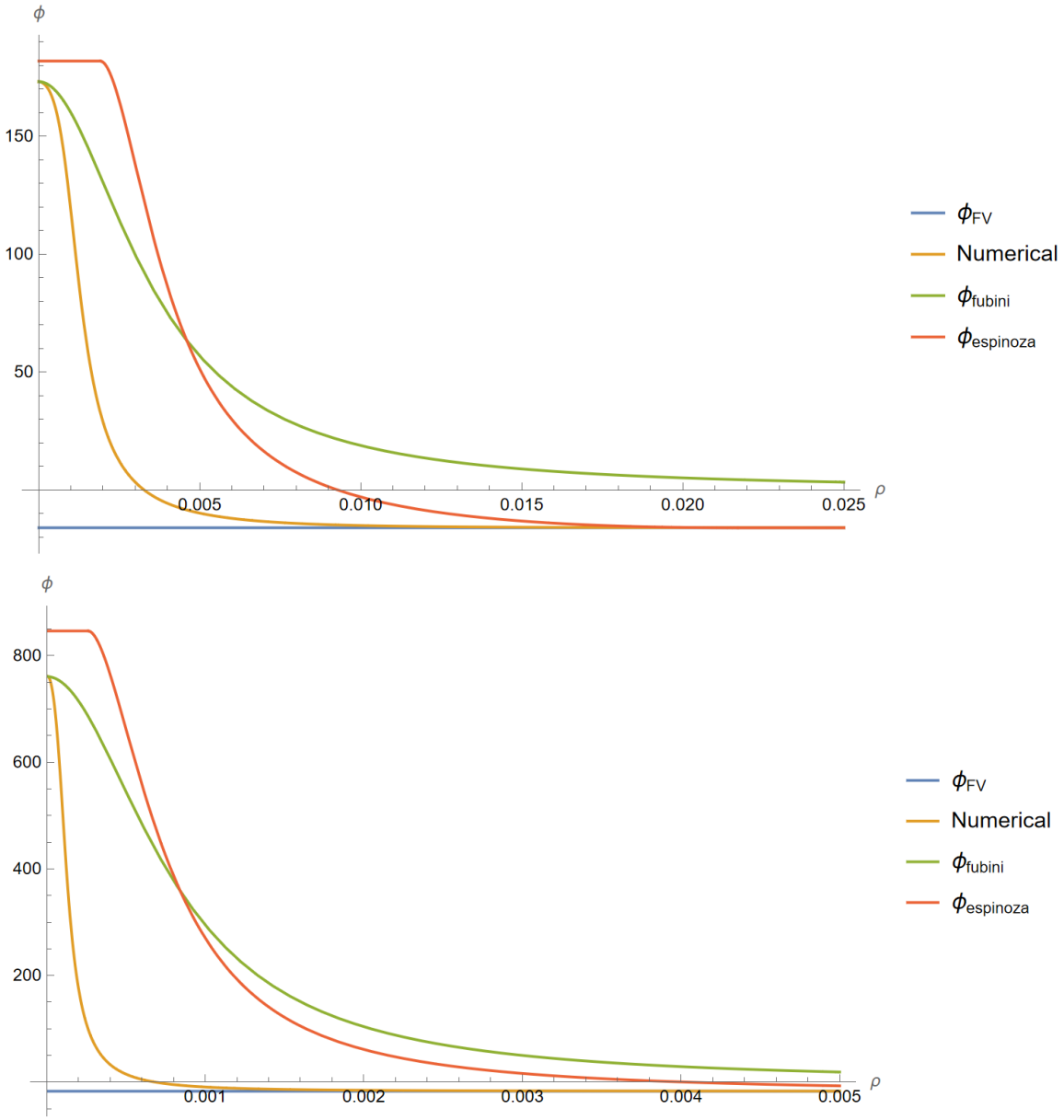

Figure 4.6: (Continued from 4.5) A comparison of several $\phi(\rho)$ profiles: those of Fubini, Espinosa, and our numerical solutions as they decay to ϕ_{FV}, with four snapshots as our ϕ_{TV} goes to ∞.

Chapter 5: Conclusion

We set out to better understand the breakdown of the Euclidean bounce approach to estimate the lifetime of the false vacuum for the $-\lambda\phi^4$ potential. For this potential, there is an infinite number of bounces, each corresponding to a different field value at the center of the nucleating bubble. The action's value is independent of the field's value at the center, rendering Coleman's approach useless to single out a decay path. Our approach uses a modified potential, $V = -\lambda\phi^4 + \alpha\phi^5 + \beta\phi^6$ that overlaps with the unstable $-\lambda\phi^4$ for a considerable range of field values around the false vacuum, $\phi = 0$. The modified potential has a unique bounce solution. We investigate how the action of the modified potential bounce changes as the true vacuum approaches a median region that follows the shape of the known unstable potential while containing a fixed false vacuum and a true vacuum that can be pushed to infinity. We contrast our approach with that of Espinosa et al. They postulate a decay path they call the pseudo-bounce that solves the Euclidean bounce equations only in a finite region of field space. To each pseudo-bounce, they associate an action, which then they extremize. We used this method as a baseline of comparison against our numerical calculation of a modified potential to understand what happens to the value of the action and the field as we asymptotically approach this region. Choosing from a table of values for our constant α, β, and λ, we expected the resultant values of B to move inversely proportional to $\Delta V = V(\phi_{\text{fv}}) - V(\phi_{\text{tv}})$; This was true for both cases of thin wall and thick wall. However we did not appear to gain any additional insight into this breakdown from our calculation. As the value of ϕ_{tv} is pushed to infinite, the value of the field at the center of the bubble stops being ϕ_{tv}, but still tracks it. As a result, the width of the tunneling barrier increases, and the action approaches

zero from above, making the decay rate of order one and the bounce approximation unreliable. If the B values had not gone to zero, this numerical method of modifying the unstable quartic potential could represent a simpler way of calculating the decay rate of a class of such potentials. Our numerical values for the Euclidean action do not quite match Espinosa's, though they follow a similar trend as the $\phi_{\text{tv}} \to \infty$. This is probably due to the contribution to the action in the region where the deformed potential differs from $-\lambda\phi^4$.

Neither method gives a reliable path for the false vacuum decay. If $-\lambda\phi^4$ is only an effective potential for small values of ϕ, then our numerical analysis shows that we must know the actual potential to estimate both the decay path and the decay rate. Espinosa et al.'s approach never agrees with the numerical result, not even in the thin-wall regime.

Harold J. Johnson A hard-working graduate student, nearing the end of this chapter of your education!

Master of Arts Harold J. Johnson is about to earn this. Congratulations!

Works Cited

Curtis G. Callan, Jr. and Sidney R. Coleman. The Fate of the False Vacuum. 2. First Quantum Corrections. *Phys. Rev. D*, 16:1762–1768, 1977. doi: 10.1103/PhysRevD.16.1762.

So Chigusa, Takeo Moroi, and Yutaro Shoji. Stability of electroweak vacuum and supersymmetric contribution to muon g − 2. *JHEP*, 11:027, 2023. doi: 10.1007/JHEP11(2023)027.

Sidney R. Coleman. The Fate of the False Vacuum. 1. Semiclassical Theory. *Phys. Rev. D*, 15:2929–2936, 1977. doi: 10.1103/PhysRevD.16.1248. [Erratum: Phys.Rev.D 16, 1248 (1977)].

J. R. Espinosa. Tunneling without Bounce. *Phys. Rev. D*, 100(10):105002, 2019. doi: 10.1103/PhysRevD.100.105002.

J. R. Espinosa. Thick wall from thin walls. *Phys. Rev. D*, 108(10):103503, 2023. doi: 10.1103/PhysRevD.108.103503.

Sergio Fubini. A New Approach to Conformal Invariant Field Theories. *Nuovo Cim. A*, 34:521, 1976. doi: 10.1007/BF02785664.

I. Yu. Kobzarev, L. B. Okun, and M. B. Voloshin. Bubbles in Metastable Vacuum. *Yad. Fiz.*, 20:1229–1234, 1974.

Andrei D. Linde. Hard art of the universe creation (stochastic approach to tunneling and baby universe formation). *Nucl. Phys. B*, 372:421–442, 1992. doi: 10.1016/0550-3213(92)90326-7.

Viatcheslav F. Mukhanov, Eliezer Rabinovici, and Alexander S. Sorin. Quantum Fluctuations and New Instantons I: Linear Unbounded Potential. *Fortsch. Phys.*, 69(2):2000100, 2021. doi: 10.1002/prop.202000100.

L. B. Okun. Vacua, vacuum: The Physics of nothing. *NATO Sci. Ser. B*, 352: 67–74, 1996. doi: 10.1007/978-1-4613-1147-8_6.

Erick J. Weinberg. *Classical solutions in quantum field theory: Solitons and Instantons in High Energy Physics*. Cambridge Monographs on Mathematical Physics. Cambridge University Press, 9 2012. ISBN 978-0-521-11463-9, 978-1-139-57461-7, 978-0-521-11463-9, 978-1-107-43805-7. doi: 10.1017/CBO9781139017787.